CHAPTER 5

MODEL VERIFICATION

To investigate the suitable equation of state for estimating the thermodynamic properties of carbon dioxide several models were investigated. Comparison between calculation results and analytical data from the Peng-Robinson EOS and the Soave Redlich-Kwong EOS were conducted for verifying their suitability.

After verifying the EOS, a set of basic mathematical model is developed and encoded as a program for simulation of rapid expansion of supercritical solution (RESS) in the two-dimensional fluidized bed system, comparison of simulation results and analytical solutions with the other researches was also carried out and discussed later.

5.1 Comparison between Peng-Robinson EOS and Soave Redlich-Kwong EOS

The relevant parameters from the simulation are listed in Table 5.1 where the inlet pressure is varied as:

- Case 1.1 – 1.4: the inlet pressure is varied between 70 – 97 bar
- Case 2.1 – 2.4: the inlet pressure is varied between 82 – 149 bar
- Case 3.1 – 3.4: the inlet pressure is varied between 94 – 203 bar
- Case 4.1 – 4.4: the inlet pressure is varied between 105 – 256 bar

Mean while Zc from the Peng-Robinson EOS is 0.307
Zc from the Soave Redlich-Kwong EOS is 0.333
Zc of the carbon dioxide is 0.274

Table 5.1 Parameters for analytical solution and simulation in this study

Case	Inlet temp.	Equation of State	Compressibility, Zc
1.1	313 K	Peng-Robinson	Zc of the Peng-Robinson
1.2			Zc of carbon dioxide
1.3		Soave Redlich-Kwong	Zc of the Soave Redlich-Kwong
1.4			Zc of carbon dioxide
2.1	333 K	Peng-Robinson	Zc of the Peng-Robinson
2.2			Zc of carbon dioxide
2.3		Soave Redlich-Kwong	Zc of the Soave Redlich-Kwong
2.4			Zc of carbon dioxide
3.1	353 K	Peng-Robinson	Zc of the Peng-Robinson
3.2			Zc of carbon dioxide
3.3		Soave Redlich-Kwong	Zc of the Soave Redlich-Kwong
3.4			Zc of carbon dioxide
4.1	373 K	Peng-Robinson	Zc of the Peng-Robinson
4.2			Zc of carbon dioxide
4.3		Soave Redlich-Kwong	Zc of the Soave Redlich-Kwong
4.4			Zc of carbon dioxide

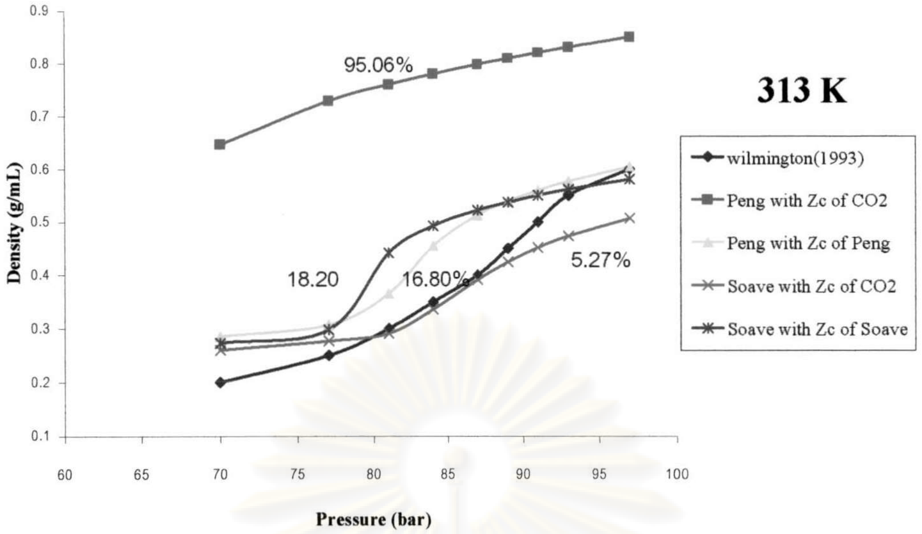

Figure 5.1 The relation between the pressure and the density of carbon dioxide calculated from Peng-Robinson Equation of State and Soave-Redlich-Kwong Equation of State and the experimental results of Wilmington, DE's work (1993) at temperature 313 K

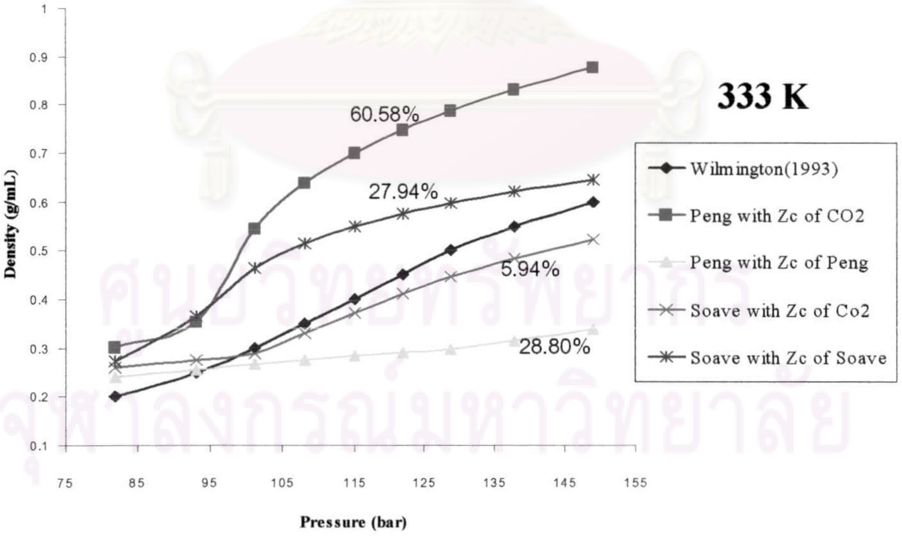

Figure 5.2 The relation between the pressure and the density of carbon dioxide calculated from Peng-Robinson Equation of State and Soave-Redlich-Kwong Equation of State and the experimental results of Wilmington, DE's work (1993) at temperature 333 K

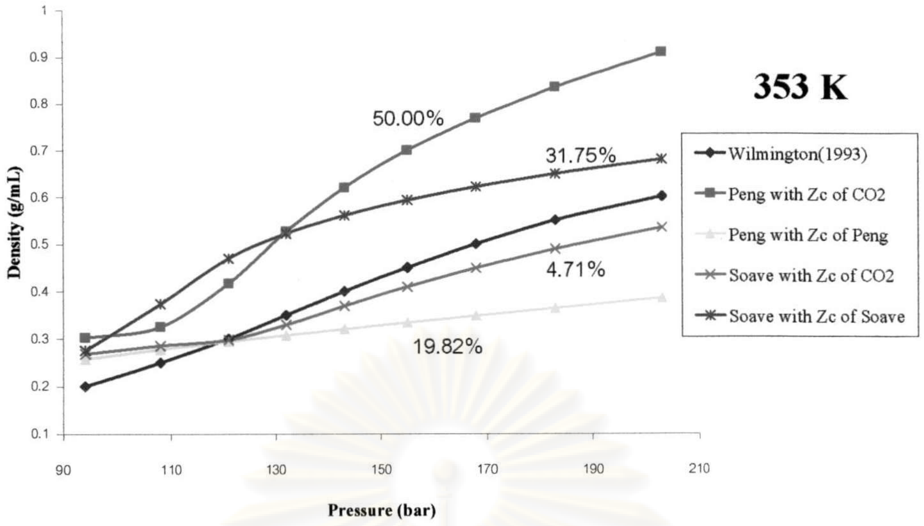

Figure 5.3 The relation between the pressure and the density of carbon dioxide calculated from Peng-Robinson Equation of State and Soave-Redlich-Kwong Equation of State and the experimental results of Wilmington, DE's work (1993) at temperature 353 K

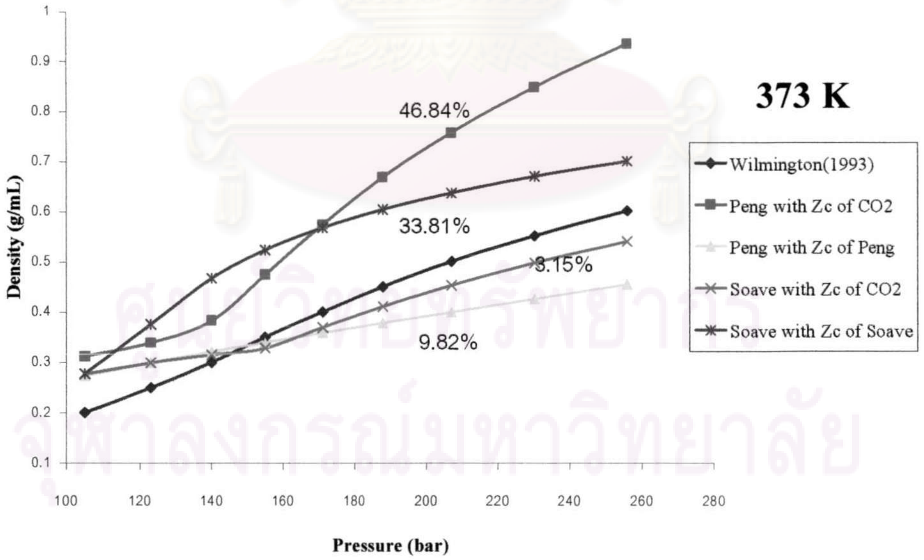

Figure 5.4 The relation between the pressure and the density of carbon dioxide calculated from Peng-Robinson Equation of State and Soave-Redlich-Kwong Equation of State and the experimental results of Wilmington, DE's work (1993) at temperature 373 K

Relative difference between the calculated results and the experimental results reported by Wilmiington (1993) were calculated by using the following equation.

$$\text{Relative difference} = [\, \Sigma\, (\rho_{exp} - \rho_{cal}) \,/\, \Sigma\, \rho_{exp} \,] * 100 \qquad (5.1)$$

According to the comparison in figure 5.1 – 5.4, it could be considered as follows,

From Figure 5.1, it can be clearly seen that Peng-Robinson EOS with Zc of 0.274 exhibits the largest difference of 95.06% relative to the experimental results of Wilmington (1993). On the other hand, Soave Redlich-Kwong EOS with Zc of 0.274 could predict the density of CO2 with the narrowest difference of 5.27% relative to the same reference. Mean while, Peng-Robinson EOS with Zc of its own (0.307) as well as Soave Redlich-Kwong EOS with Zc of its own (0.333) could provide the calculation results with moderate difference of 16.8% and 18.2%, respectively.

Similarly, as shown in Figure 5.2 to 5.4, Soave Redlich-Kwong EOS with Zc of CO_2 (0.274) could provide the smallest difference of CO_2 density relative to the reference data. Moreover, it is noteworthy that the higher temperature, the smaller difference could be obtained from the Soave Redlich-Kwong EOS in corporate with the critical compressibility factor of CO_2 itself.

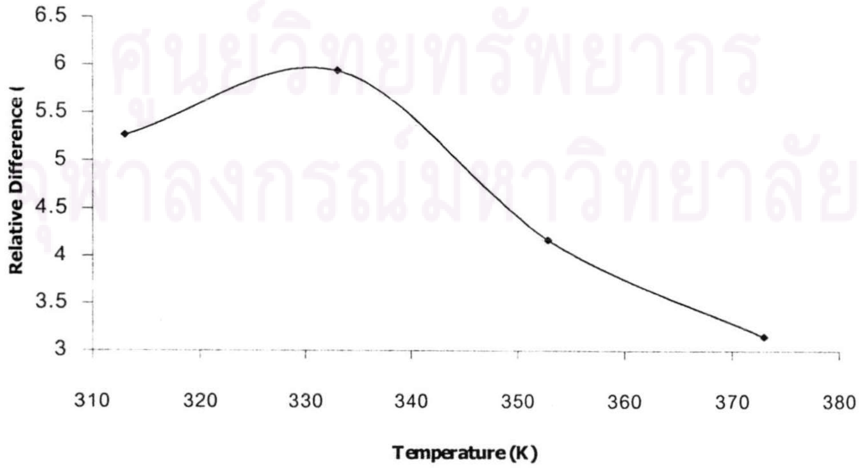

Figure 5.5 Temperature dependence of relative difference of CO_2 density predicted by Soave Redlich-Kwong EOS with Zc of CO_2

With the increasing temperature, the density of CO_2 would gradually increase because it becomes the supercritical fluid. Under such conditions, pressure will play more important role in controlling the density and other thermodynamic properties of CO_2.

It should also be noted that an increase in pressure results in the increasing density. In figure 5.1, with the temperature of 313 K in the vicinity of critical pressure of CO_2, the increase pressure could result in the drastically increasing density of CO_2. But with the higher temperature, say 353 or 373 K, as shown in Figure 5.3 and 5.4 regarding to the available data, the increase in pressure could give rise to a gradual increase in the CO_2 density.

5.2 Verification of the developed simulation model incorporated with the investigated EOS

Aim of this part is to investigate on the suitability of the fluid flow model developed for describing the rapid expansion of supercritical carbon dioxide in a two-dimensional domain by taking into account the Soave Redlich-Kwong EOS, which is previously proved that it could predict thermodynamic properties of the investigated fluid. For verification, investigated results reported by Reverchon and Pallado (1996) have been employed for comparison with the simulation result obtained in this work.

To illustrate the reference system considered by Reverchon and Pallado (1996), a schematic representation is shown in figure 5.6. The expanding fluid was accelerated from the pre-expansion conditions up to the supersonic free-jet in the post-expansion chamber. The initial velocity of the supercritical solution in the pre-expansion chamber was assumed to be negligible. At the exit, sonic conditions were reached and flow was choked.

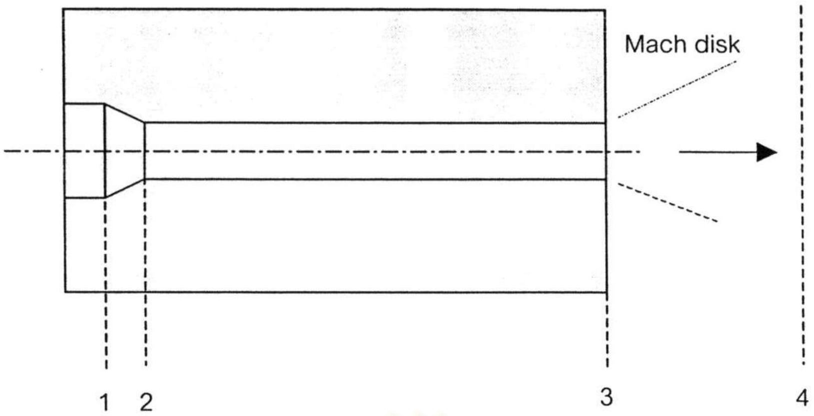

Figure 5.6 Simplified scheme of the expansion nozzle:
Capillary inlet (1-2)
Capillary duct (2-3)
Expansion chamber (3-4)

The numerical model was checked in the calculation of free-jet of supercritical carbon dioxide maintained at a constant temperature. Ten simulations were performed depending on the upstream flow conditions shown in Table 5.2

Table 5.2 Calculation conditions of employed in Reverchon and Pallado's work.

Cases	Upstream boundary	
	Pressure (bar)	Temperature (K)
1	200	333
2	200	353
3	200	373
4	260	333
5	260	353
6	260	373

Initial conditions:

- Temperature = 298 K
- Pressure = 1 bar
- X-direction velocity = 0.0 m/s
- Y-direction velocity = 0.0 m/s
- Nozzle diameter = 40d-6 m

Boundary Condition

- At the nozzle wall, no slip conditions
- Nozzle was heated for constant temperature at the inlet temperature of fluid
- At the downstream boundary of the computation domain was imposed that a no slip boundary condition and there exists an adiabatic flat plate.

Table 5.3 Simulation conditions used in the explicit finite difference simulations.

Simulation conditions	
Number of grid points in the y, z directions	24 x 521
Grid size ($\Delta y, \Delta z$)	1d-5, 4d-5 m
Interval time	5000000
Integration step size(Δt)	1.0d-14 sec.
Specific gas constant of CO_2	8.314*1000/44.01
Ratio of specific heat of CO_2	1.304
Prandtl number	0.710
Bed pressure of fluid	1.0 bar
Bed temperature of fluid	298.0 K
Bed density of fluid	5.30778d-3 kg/m^3
Reference Temperature	293.0 K
Reference viscosity of CO_2 at Trf	1.463d-4 kg/(m·s)

Table 5.4 Simulation conditions used in the implicit finite difference simulations.

Simulation conditions	
Number of grid points in the y, z directions	24 x 521
Grid size ($\Delta y, \Delta z$)	1d-5, 4d-5 m
Interval time	250000
Integration step size(Δt)	2.0d-13 sec.
Specific gas constant of CO_2	8.314*1000/44.01
Ratio of specific heat of CO_2	1.304
Prandtl number	0.710
Bed pressure of fluid	1.0 bar
Bed temperature of fluid	298.0 K
Bed density of fluid	5.30778d-3 kg/m^3
Reference Temperature	293.0 K
Reference viscosity of CO_2 at Trf	1.463d-4 kg/(m·s)

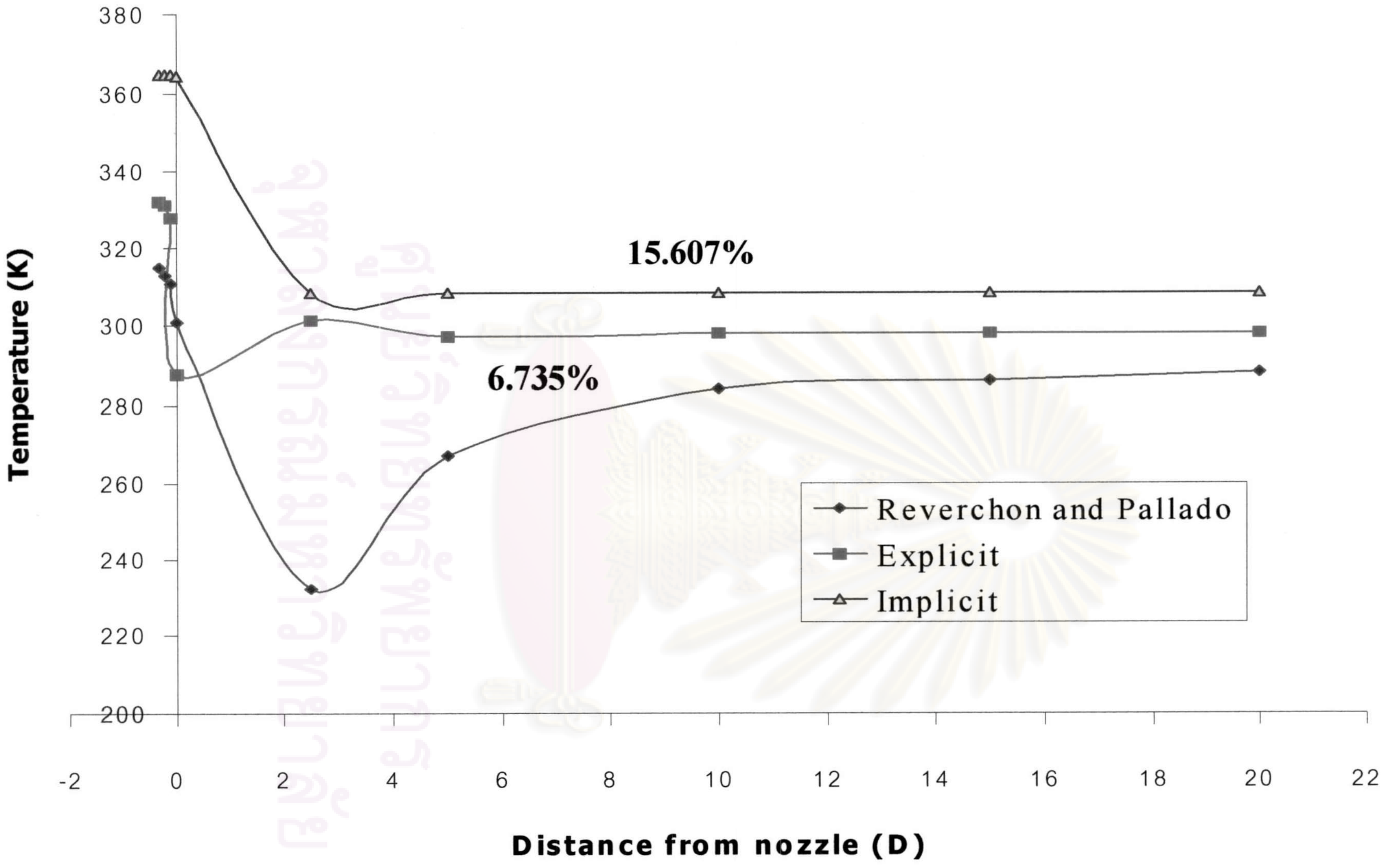

Figure 5.7 Relative graph of temperature and distance from nozzle at inlet pressure 200 bar and inlet temperature 333 K

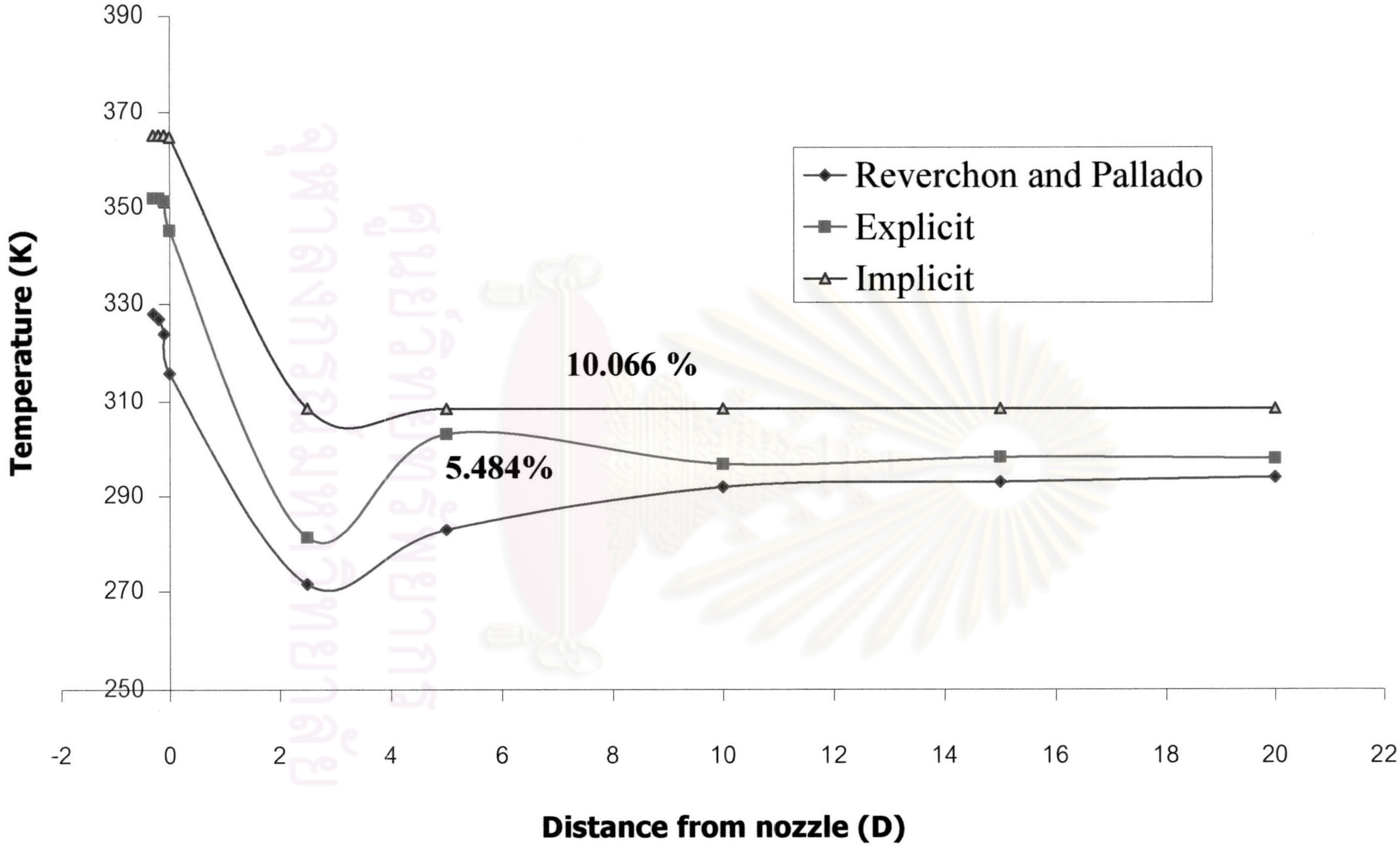

Figure 5.8 Relative graph of temperature and distance from nozzle at inlet pressure 200 bar and inlet temperature 353 K

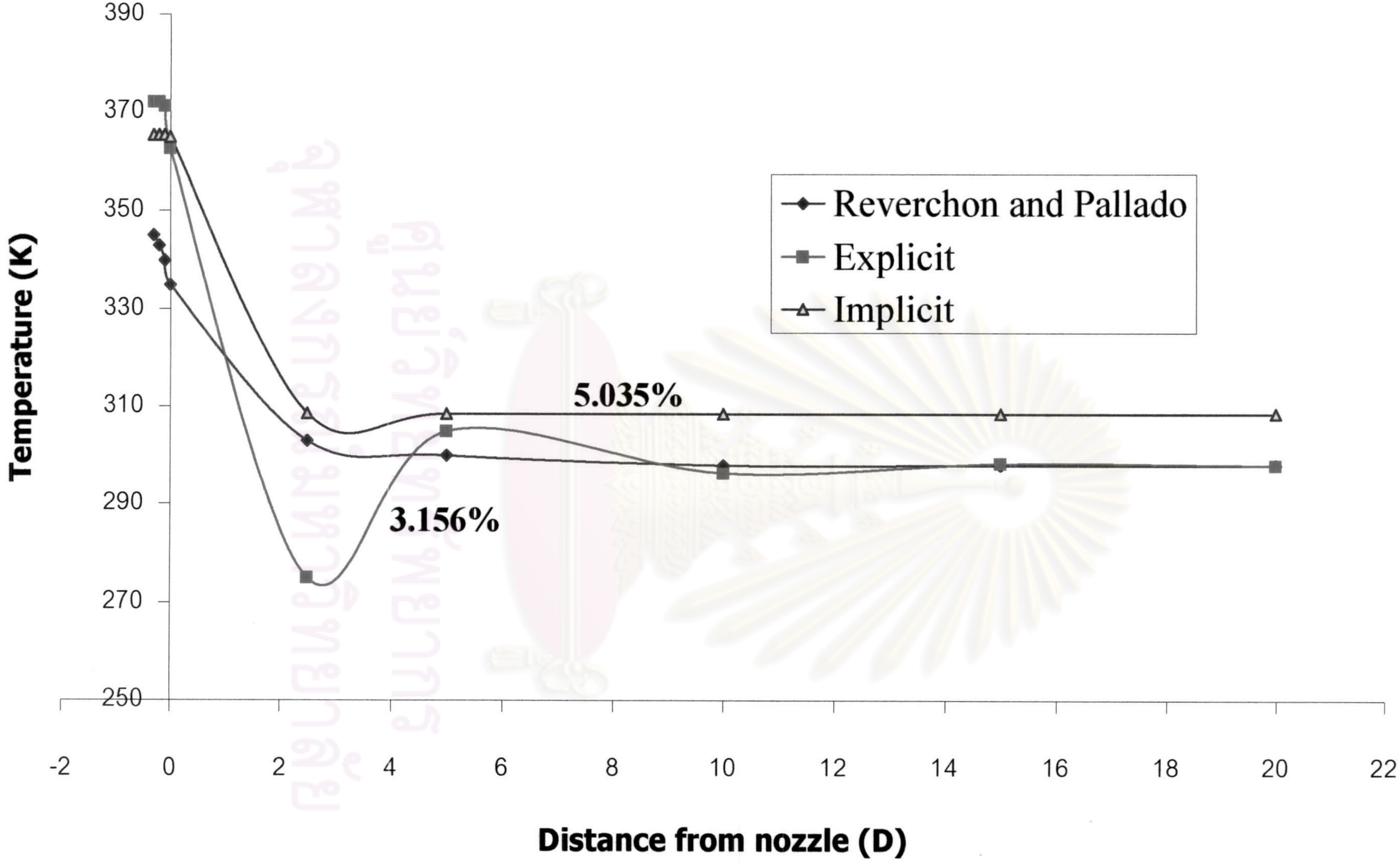

Figure 5.9 Relative graph of temperature and distance from nozzle at inlet pressure 200 bar and inlet temperature 373 K

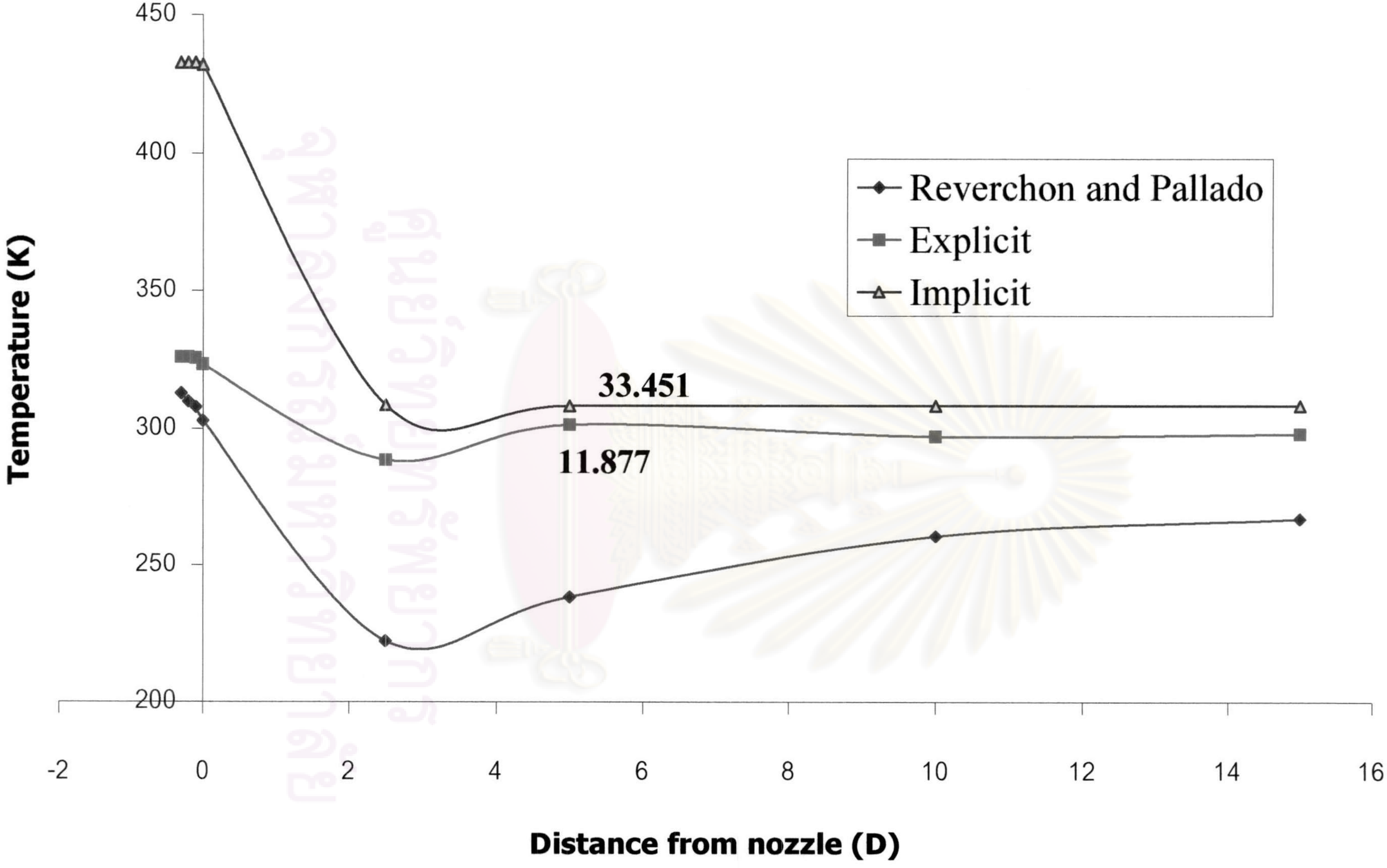

Figure 5.10 Relative graph of temperature and distance from nozzle at inlet pressure 260 bar and inlet temperature 333 K

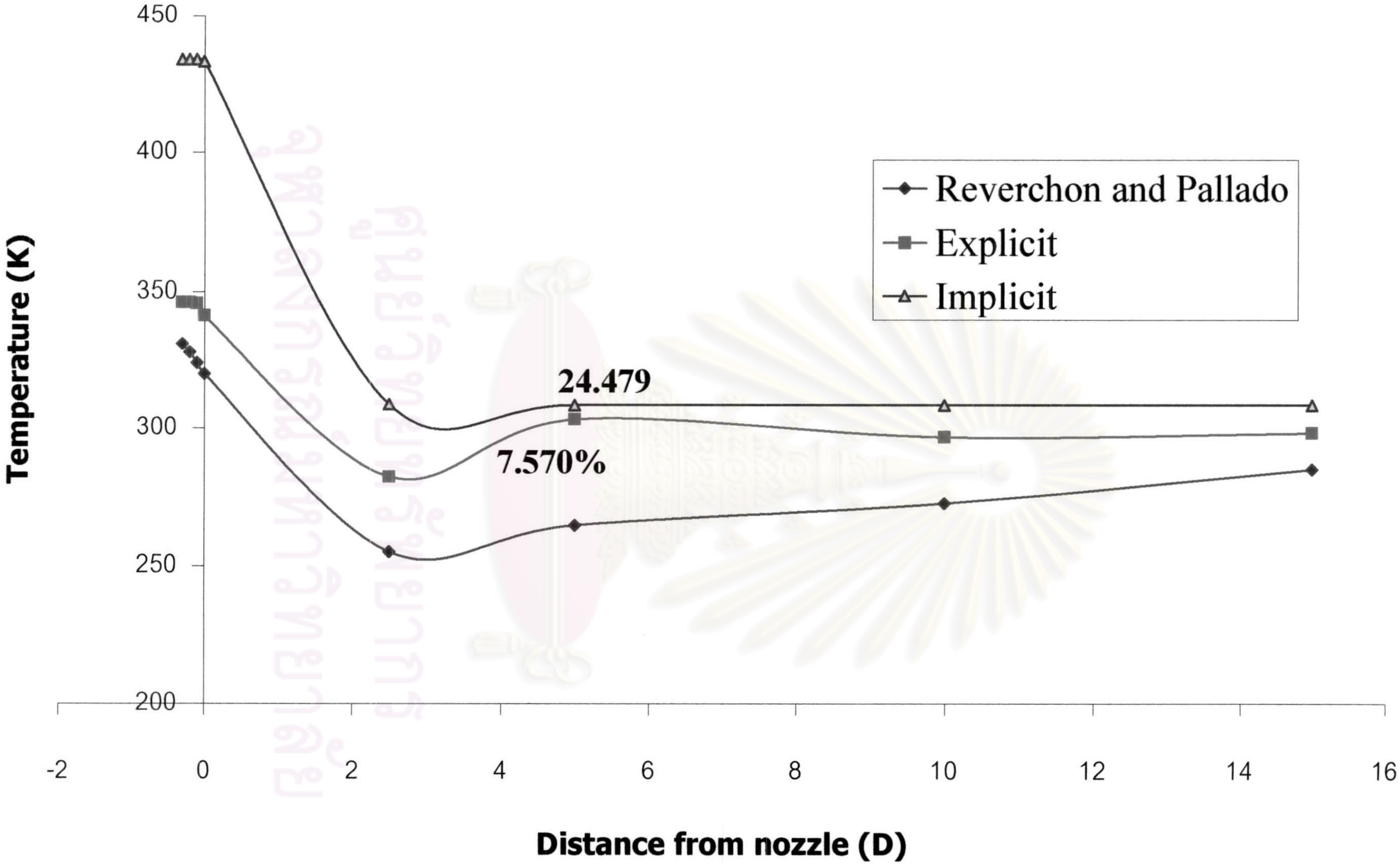

Figure 5.11 Relative graph of temperature and distance from nozzle at inlet pressure 260 bar and inlet temperature 353 K

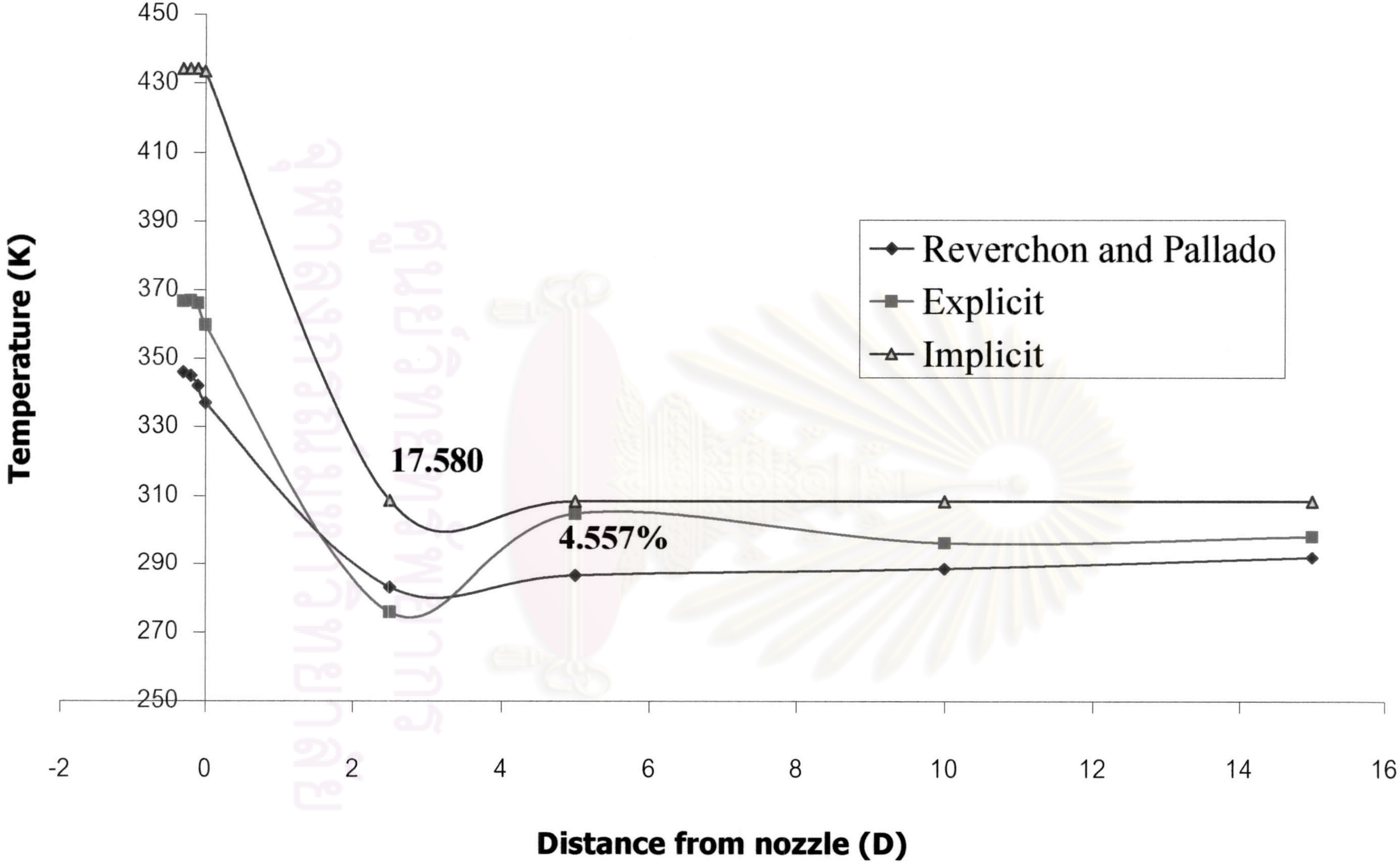

Figure 5.12 Relative graph of temperature and distance from nozzle at inlet pressure 260 bar and inlet temperature 373 K

From Reverchon and Pallado (1996)'s work. It could be clearly seen that temperature of fluid drastically decreases after it is ejected out of the nozzle. After the fluid flows along a certain distance out of the nozzle tip, temperature of the fluid becomes slightly recovered and there remains constant at the certain level. This could be considered that the fluid reaches its thermal equilibrium due to heat transfer with the surrounding. However, on increase in the inlet temperature of fluid results in a gradual decrease in temperature of the flowing fluid.

An increase in the inlet pressure of the fluid also affected the temperature profile along in calculating domain. The decrease in temperature of the fluid became steeper especially under the condition of lower inlet temperature.

Relative difference between the calculated results and the simulated results reported by Reverchon and Pallado (1996) were calculated by using the following equation.

$$\text{Relative difference} = [\, \Sigma\, (\rho_{sim} - \rho_{cal}) \,/\, \Sigma\, \rho_{sim} \,] * 100 \qquad (5.2)$$

Table 5.5 Calculated Percent Relative difference.

Cases	Upstream boundary		Relative difference (%)	
	Pressure (bar)	Temperature (K)	Explicit	Implicit
1	200	333	6.73539	15.60728
2	200	353	5.48423	10.06599
3	200	373	3.15620	5.03538
4	260	333	11.87683	33.45141
5	260	353	7.57030	24.74887
6	260	373	4.55736	17.85016

According to the comparison in figure 5.7 – 5.12, it could be considered as follows,

The simulation results obtained from a program code which is developed from a set of basic equations of fluid flow incorporated with Soave Redlich-Kwong EOS exhibited a consistent trend compared with reference. The conditions considered are the same as Reverchon and Pallado's work. It could be clearly seen that in the vicinity of nozzle tip both before and after ejection, temperature of fluid decreases sharply. These phenomena could be implied as the Joule-Thompson effect. After decreasing temperature rises rapidly again due to the heat transfer between the flowing fluid and environment.

These results agree well with the those of Reverchon and Pallado's work. However, there is a distinct difference which is an overshooting of temperature at the downstream distance equal to the nozzle diameter. This could be implied as the dependence of the explicit method. Anyway, finally the fluid temperature converts to a constant level after the fluid flow far enough from the nozzle.

On the other hand, implicit approach was also employed for simulation. Basically, the simulation results show an agreement with those of Reverchon and Pallado's work or those of explicit simulation. However, this implicit simulation could be not exhibit the clear effect of the inlet temperature as could be seen from explicit simulation. This could be implied as results of deficiency of the program code developed in this work. Basically, the implicit method should provide the same on better results compared with that of the explicit method. Many effects have been spent for solving the deficiency problem but it has not been succeeded yet. Therefore, it is inevitably necessary to use the explicit simulation for investigating effect of other parameters on rapid expansion of supercritical carbon dioxide phenomena of which simulation results will be discuss later in chapter 6.